Joint Optimization of Transmit and Receive Beamforming in Active Arrays

Jun Liu, *Member, IEEE*, Hongbin Li, *Senior Member, IEEE*, and Braham Himed, *Fellow, IEEE*

***Abstract*—We jointly design the transmit and receive beamforming based on a-priori information on the locations of target and interferences in an active array, where each transmit element emits the same waveform up to a complex scalar. A sequential optimization algorithm is proposed to maximize the output signal-to-interference-plus-noise ratio (SINR). Numerical results demonstrate that a significant gain in the output SINR can be achieve in this active array, compared to the conventional phased-array radar and omnidirectional multiple-input-multiple-output (MIMO) radar.**

***Index Terms*—Active array, optimization, receive beamforming, receive filter, transmit beamforming.**

I. Introduction

An ACTIVE system has the capability of judiciously selecting its transmit waveform and receiver processing strategy based on a-priori knowledge about the target and environment, in order to maximize its detection and estimation performance. There has been a growing interest in jointly designing transmit waveforms and receive filters in active radar, sonar, and communication systems [1]–[6].

In [3], the enhancement in detection performance is obtained through designing the complex amplitudes of a coherent burst of pulses of a monostatic radar system under similarity constraints. Furthermore, a similar problem is considered in [4] and [5] by adding the constraints of phase-only modulation and peak-to-average-power ratio, respectively. Recently, a sequential optimization algorithm is proposed to combine the design of transmit signal and the optimization of receive filter to achieve significant improvements in output signal-to-interference-plus-noise ratio (SINR) [2]. In order to minimize the mean square error in estimating the radar cross section of a target, the authors in [6] optimize both transmit codes and receive filters. Notice that at the transmit design stage, the work mentioned above focuses on optimizing the temporal codes of the transmit waveform in the temporal domain. When an active array is employed, we can consider the design of weights on each transmit element, i.e., optimizing the transmit beamforming in the spatial domain.

In the conventional phased-array (PA) radar, each transmit element sends out a phase-shifted version of a single waveform in order to achieve directional transmission towards the target of interest. This strategy, regardless of interferences, concentrates all transmit powers on the target of interest, and thus obtains a directional gain in the direction of target echo. It is proven in [7] that the PA radar maximizes the signal-to-noise ratio (SNR). However, it does not mean that the PA radar can output the optimal SINR in an environment where interferences exist. In such environment, the radar system is expected to adjust its transmit waveform and receive filter to match the target and at the same time null the interferences, in order to operate optimally.

We examine herein the problem of maximizing the output SINR by jointly designing the transmit and receive beamformers with a-priori knowledge about the locations of target and interferences in an active array, where each element transmits a scaled (both in amplitude and phase) version of a single waveform. An iterative algorithm is employed to design the transmit and receive beamformers such that the output SINR is maximized. Simulation results reveal that the active array employing the proposed optimization algorithm can handle more interferences and show superiority in suppressing interferences with respect to the conventional PA radar. Moreover, it is shown that such active array can output the highest SINR, compared to the conventional PA and omnidirectional multiple-input-multiple-output (MIMO) radars.

Notation: Vectors (matrices) are denoted by boldface lower (upper) case letters, all vectors are column vectors, superscripts $(\cdot)^T$ and $(\cdot)^\dagger$ denote transpose and complex conjugate transpose, respectively, $E\{\cdot\}$ denotes statistical expectation, $\mathbf{I}$ is the identity matrix, $|\cdot|$ represents the modulus of a complex number, and $\|\cdot\|$ is the Euclidean norm of a vector.

II. Problem Formulation

Consider a radar system with N_t co-located transmit elements and N_r co-located receive elements. A beamforming vector $\mathbf{t} = [t_1, t_2, \ldots, t_{N_t}]^T$ is designed to transmit a waveform $s(l), l = 1, 2, \ldots, L$ where L denotes the number of samples, with a beamforming weight of t_n on the nth element. This is to say, the baseband equivalent, in complex-valued form, of the transmitted signals from the N_t transmit elements can be expressed as

$$\mathbf{t}s(l), \quad l = 1, 2, \ldots, L, \tag{1}$$

where $\|\mathbf{t}\| = 1$. Note that the amplitude and phase of each entry in $\mathbf{t}$ can be designed as long as the norm of $\mathbf{t}$ is unit. It is obvious that this radar system includes the PA radar as a special case. For

Manuscript received July 22, 2013; revised October 30, 2013; accepted October 31, 2013. Date of publication November 06, 2013; date of current version November 14, 2013. This work was supported in part by a subcontract with Dynetics, Inc. for research sponsored by the Air Force Research Laboratory (AFRL) under Contract FA8650-08-D-1303 . The associate editor coordinating the review of this manuscript and approving it for publication was Prof. Shahram Shahbazpanahi.

J. Liu and H. Li are with the Department of Electrical and Computer Engineering, Stevens Institute of Technology, Hoboken, NJ 07030 USA (e-mail: jun_liu_math@hotmail.com; hongbin.li@stevens.edu).

B. Himed is with RF Technology Branch, Air Force Research Laboratory, AFRL/RYMD, Wright-Patterson Air Force Base, Dayton, OH 45433 USA (e-mail: braham.himed@wpafb.af.mil).

Color versions of one or more of the figures in this paper are available online at http://ieeexplore.ieee.org.

Digital Object Identifier 10.1109/LSP.2013.2289325

a uniform linear array (ULA) with d inter-element separation, $\mathbf{t}$ has the following form

$$\mathbf{t} = \frac{1}{\sqrt{N_t}}\left[1, \mathrm{e}^{-j\frac{2\pi d}{\lambda}\sin\theta_0}, \ldots, \mathrm{e}^{-j(N_t-1)\frac{2\pi d}{\lambda}\sin\theta_0}\right]^T, \quad (2)$$

where θ_0 is the look direction of a target and λ denotes the wavelength.

The signal seen at a specific location with angle θ in the far field is a superposition of the delayed and attenuated version of the transmitted signals. Throughout this paper, we assume a narrowband system such that the signal seen at that location is given by [8, chap. 6]

$$\mathbf{a}_t^T(\theta)\mathbf{t}s(l-\tau), \quad l = 1, 2, \ldots, L, \quad (3)$$

where $\mathbf{a}_t(\theta) \in \mathbb{C}^{N_t}$ is a steering vector containing the phase shifts due to propagation, and τ denotes a propagation delay to the waveform. For a ULA with d inter-element separation, $\mathbf{a}_t(\theta)$ takes the form

$$\mathbf{a}_t(\theta) = \left[1, \mathrm{e}^{-j\frac{2\pi d}{\lambda}\sin\theta}, \ldots, \mathrm{e}^{-j(N_t-1)\frac{2\pi d}{\lambda}\sin\theta}\right]^T. \quad (4)$$

Suppose there are N_i interference sources located at the look directions $\theta_i \neq \theta_0$, $i = 1, 2, \ldots, N_i$. The baseband equivalent of the received signals are given by

$$\begin{aligned}\mathbf{x}(l) &= \tilde{\alpha}_0\mathbf{a}_r(\theta_0)\mathbf{a}_t^T(\theta_0)\mathbf{t}s(l-2\tau_0) \\ &\quad + \sum_{i=1}^{N_i}\tilde{\alpha}_i\mathbf{a}_r(\theta_i)\mathbf{a}_t^T(\theta_i)\mathbf{t}s(l-2\tau_i) + \tilde{\mathbf{n}}(l), \quad (5)\end{aligned}$$

where $\tilde{\alpha}_0$ and $\tilde{\alpha}_i$ are the complex amplitudes of the target and the ith interference, respectively, $2\tau_0$ and $2\tau_i$ are the delays of the target and the ith interference, respectively, $\mathbf{a}_r(\theta)$ denotes an $N_r \times 1$ steering vector of phase shifts due to the propagation from a source to the receive elements, and $\tilde{\mathbf{n}}(l)$ signifies an $N_r \times 1$ additive white Gaussian noise vector. The vector $\mathbf{a}_r(\theta)$, which is similarly defined as $\mathbf{a}_t(\theta)$ in (4), is usually referred to as the receive steering vector. Note that when the transmit and receive arrays are not co-located, the look and receive angles are different. However, since the relative positions of the two arrays are typically known, the same directional variable is used for notational convenience.

The received signal is processed by a matched filter aligned to the target delay, which outputs [9]

$$\mathbf{y} = \alpha_0\mathbf{A}(\theta_0)\mathbf{t} + \sum_{i=1}^{N_i}\alpha_i\mathbf{A}(\theta_i)\mathbf{t} + \mathbf{n}, \quad (6)$$

where $\mathbf{A}(\theta) = \mathbf{a}_r(\theta)\mathbf{a}_t^T(\theta)$, α_0 and α_i are the complex amplitudes of the target and the ith interference after the matched filter, respectively, and the noise $\mathbf{n}$ has zero mean and covariance matrix $\sigma_n^2\mathbf{I}$. Assume also that α_i's are mutually uncorrelated with zero mean and variance σ_i^2. The vector of observation $\mathbf{y}$ is filtered through the weight vector $\mathbf{w}$, and then the output SINR can be expressed as

$$\mathrm{SINR} = \frac{\sigma_0^2\left|\mathbf{w}^\dagger\mathbf{A}(\theta_0)\mathbf{t}\right|^2}{\mathbf{w}^\dagger\mathbf{R}_\mathbf{t}\mathbf{w} + \mathbf{w}^\dagger\mathbf{w}\sigma_n^2}, \quad (7)$$

where $\mathbf{R}_\mathbf{t} = E\{\mathbf{c}\mathbf{t}\mathbf{t}^\dagger\mathbf{c}^\dagger\}$, with $\mathbf{c} = \sum_{i=1}^{N_i}\alpha_i\mathbf{A}(\theta_i)$. The receive filter $\mathbf{w}$ is also referred to as the receive beamformer. In the following, we aim to jointly design the transmit beamformer $\mathbf{t}$ and the receive beamformer $\mathbf{w}$ in order to maximize SINR given knowledge of the interferences (locations and strengths). This is equivalent to the following optimization problem:

$$\begin{cases}\max\limits_{\mathbf{t},\mathbf{w}} \frac{|\mathbf{w}^\dagger\mathbf{A}(\theta_0)\mathbf{t}|^2}{\mathbf{w}^\dagger\mathbf{R}_\mathbf{t}\mathbf{w}+\mathbf{w}^\dagger\mathbf{w}\sigma_n^2} \\ \text{s.t.} \quad \|\mathbf{t}\| = 1\end{cases}. \quad (8)$$

III. Joint Design of $\mathbf{t}$ and $\mathbf{w}$

In this section, a sequential optimization algorithm similar to that of [10] is employed to solve (8), namely, we first optimize $\mathbf{w}$ for a fixed $\mathbf{t}$ and then optimize $\mathbf{t}$ for a fixed $\mathbf{w}$. This approach is also used in [2]. More specifically, we first solve $\mathbf{w}$ for a given $\mathbf{t}$. The optimization problem can be written as

$$\max_{\mathbf{w}} \frac{|\mathbf{w}^\dagger\mathbf{A}(\theta_0)\mathbf{t}|^2}{\mathbf{w}^\dagger\mathbf{R}_\mathbf{t}\mathbf{w} + \mathbf{w}^\dagger\mathbf{w}\sigma_n^2}. \quad (9)$$

Further, the optimization problem in (9) can be recast as the well-known minimum variance distortionless response (MVDR) problem [11], i.e.,

$$\begin{cases}\min\limits_{\mathbf{w}} \mathbf{w}^\dagger(\mathbf{R}_\mathbf{t} + \sigma_n^2\mathbf{I})\mathbf{w} \\ \text{s.t.} \quad \mathbf{w}^\dagger\mathbf{A}(\theta_0)\mathbf{t} = 1\end{cases}. \quad (10)$$

It is easy to obtain the optimal $\mathbf{w}$ in (10) to be

$$\mathbf{w} = \beta(\mathbf{R}_\mathbf{t} + \sigma_n^2\mathbf{I})^{-1}\mathbf{A}(\theta_0)\mathbf{t}, \quad (11)$$

where β is a scalar satisfying the equality constraint. Note that the scalar can be ignored because it has no effect on the original objective function in (9).

After obtaining the receive beamformer $\mathbf{w}$, we now solve for $\mathbf{t}$ in terms of $\mathbf{w}$. For a fixed $\mathbf{w}$, the optimal transmit beamformer $\mathbf{t}$ can be obtained by solving the following optimization problem:

$$\begin{cases}\max\limits_{\mathbf{t}} \frac{|\mathbf{w}^\dagger\mathbf{A}(\theta_0)\mathbf{t}|^2}{\mathbf{t}^\dagger\mathbf{R}_\mathbf{w}\mathbf{t}+\mathbf{w}^\dagger\mathbf{w}\sigma_n^2} \\ \text{s.t.} \quad \|\mathbf{t}\| = 1\end{cases}, \quad (12)$$

where $\mathbf{R}_\mathbf{w} = E\{\mathbf{c}^\dagger\mathbf{w}\mathbf{w}^\dagger\mathbf{c}\}$. According to Proposition 1 in [10], the optimization problem in (12) is equivalent to

$$\begin{cases}\max\limits_{\mathbf{t}} \frac{|\mathbf{w}^\dagger\mathbf{A}(\theta_0)\mathbf{t}|^2}{\mathbf{t}^\dagger(\mathbf{R}_\mathbf{w}+\sigma_n^2\mathbf{w}^\dagger\mathbf{w}\mathbf{I})\mathbf{t}} \\ \text{s.t.} \quad \|\mathbf{t}\| = 1\end{cases}. \quad (13)$$

It is straightforward that the optimal $\mathbf{t}$ for (13) is

$$\mathbf{t} = \gamma(\mathbf{R}_\mathbf{w} + \sigma_n^2\mathbf{w}^\dagger\mathbf{w}\mathbf{I})^{-1}\mathbf{A}^\dagger(\theta_0)\mathbf{w}, \quad (14)$$

where γ is a scalar to ensure the unit norm of $\mathbf{t}$. The above sequential optimization algorithm is stopped when the SINR improvement is no more than a pre-assigned number δ (e.g., $\delta = 10^{-6}$). It is obvious that the objective function is bounded and nondecreasing in each iteration. The above iterative algorithm will converge due to the monotone convergence theorem.

Nevertheless, it is not guaranteed to converge to a global optimum. It is shown in [10] that the solution obtained by the iterative algorithm is better than a local maximum.

Finally, the above iterative optimization procedures are summarized in the flow chart below.

Algorithm 1:

Input: $\mathbf{A}(\theta_0)$, $\mathbf{c}$, σ_n^2

Output: A solution $(\mathbf{t}^*, \mathbf{w}^*)$ of (8)

0: set $n = 0$, randomly select $\mathbf{t}_{(n)} := \mathbf{t}_0$;

1: $\mathbf{R}_{\mathbf{t}}^{(n)} := \mathrm{E}\{\mathbf{c}\mathbf{t}_{(n)}\mathbf{t}_{(n)}^\dagger\mathbf{c}^\dagger\}$;

2: $\mathbf{w}_{(n)} := [\mathbf{R}_{\mathbf{t}}^{(n)} + \sigma_n^2\mathbf{I}]^{-1}\mathbf{A}(\theta_0)\mathbf{t}_{(n)}$;

3: use (7) to compute $\mathrm{SINR}_1^{(n)}$;

4: $\mathbf{R}_{\mathbf{w}}^{(n)} := \mathrm{E}\{\mathbf{c}^\dagger\mathbf{w}_{(n)}\mathbf{w}_{(n)}^\dagger\mathbf{c}\}$;

5: $\mathbf{t}_{(n)} := [\mathbf{R}_{\mathbf{w}}^{(n)} + \sigma_n^2\mathbf{w}_{(n)}^\dagger\mathbf{w}_{(n)}\mathbf{I}]^{-1}\mathbf{A}^\dagger(\theta_0)\mathbf{w}_{(n)}$;

6: $\mathbf{t}_{(n)} := \mathbf{t}_{(n)}/\|\mathbf{t}_{(n)}\|$;

7: use (7) to compute $\mathrm{SINR}_2^{(n)}$;

8: set $n := n + 1$;

9: repeat Step 1–Step 7;

10: until $\mathrm{SINR}_2^{(n)} - \mathrm{SINR}_1^{(n)} \le \delta$;

11: output $\mathbf{t}^* := \mathbf{t}_{(n)}$ and $\mathbf{w}^* := \mathbf{w}_{(n)}$.

The overall computational complexity of the proposed algorithm is linear with respect to the number of iterations, and the complexity of each iteration is in the order of $\mathcal{O}(\max(N_t^3, N_r^3))$ [12] due to the computation of the inverse matrices in Steps 2 and 5.

It should be noted that the output of the above iterative optimization algorithm is sensitive to the choice of the initial transmit beamformer $\mathbf{t}_0$. In practice, we can perform this algorithm with a large number of random realizations of the transmit beamformer $\mathbf{t}$, and then select the optimal $(\mathbf{t}^*, \mathbf{w}^*)$ corresponding to the maximum output SINR.

IV. Simulation Results

In this section, numerical simulations are provided. For comparison purposes we consider two well-known beamformers in the PA or omnidirectional MIMO radar, i.e., MVDR beamformer [11], and the linearly constrained minimum variance (LCMV) beamformer [13]. In the PA radar, each transmit element emits a phase-shifted version of a single waveform, which enables it to obtain a directional gain. In the omnidirectional MIMO radar, each transmit element sends out a different waveform via omnidirectional transmission [9]. The total transmission powers are assumed identical in the different radar systems for fair comparison.

Suppose that the transmitter and receiver share a ULA of $N_t = N_r = N$ elements with a half-wavelength spacing. Here, we choose $N = 5$. Assume further that the direction of arrival (DOA) of the target of interest is 30°, and the power of each interference is identical. The interference-to-noise ratio (INR) and SNR are defined as $\mathrm{INR} = 10\log_{10}\sigma_1^2/\sigma_n^2$ and $\mathrm{SNR} = 10\log_{10}\sigma_0^2/\sigma_n^2$, respectively. In the following simulations, we set $\delta = 10^{-6}$ and perform the proposed algorithm for 200 different random initializations of the transmit beamformer t, and then choose the solution $(\mathbf{t}^*, \mathbf{w}^*)$ that corresponds to the maximum output SINR.

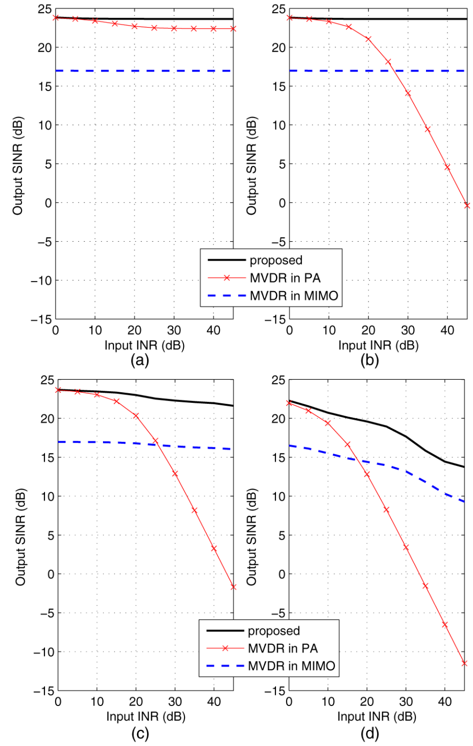

Fig. 1. Comparisons of the output SINR. (a) $N_i = 4$; (b) $N_i = 5$; (c) $N_i = 8$; (d) $N_i = 9$.

The output SINRs obtained by the proposed algorithm and the MVDR beamformer are compared for $N_i = 4, 5, 8$ and 9 in Fig. 1, where SNR = 10 dB, and the DOAs of 9 interferences are 80°, 60°, 0°, −20°, −40°, −60°, −80°, −70°, 48°. For each value of N_i, the first N_i angles in the list are used in our simulation. It can be seen from Fig. 1 that the proposed algorithm always achieves the maximum output SINR. Comparing Fig. 1(a) to Fig. 1(b), we can observe that when the number of interference signals varies from 4 to 5, the output SINR of the PA radar dramatically decreases in the high INR region. This is because the PA radar with $N = 5$ antennas has $N = 5$ degrees of freedom (DOFs), and can suppress at most $N - 1 = 4$ interference signals. As shown in Fig. 1(a)–(c), however, our proposed algorithm can effectively deal with as many as 8 interference signals. When $N_i = 9$ as illustrated in Fig. 1(d), there is also significant degradation in the output SINR of the proposed algorithm. This phenomenon can be explained using the concept of sum co-array [14]. In fact, the sum co-array for the system described in Section II has $2N - 1 = 9$ DOFs, and hence can handle at most $2N - 2 = 8$ interference signals. Notice that the MIMO radar has the same number of DOFs (i.e., $2N - 1 = 9$) as the system descried in Section II. However, the former outputs lower SINR than the latter due to the omnidirectional transmission of the MIMO radar.

With a-priori knowledge about the locations of target and interferences, it is logical to use the LCMV beamformer in the PA or omnidirectional MIMO radar case. It should be pointed out that we also conducted simulations with LCMV beamformers.

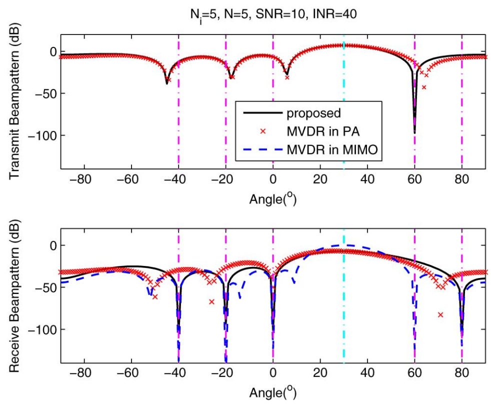

Fig. 2. Transmit and receive beampatterns for $N_i = 5$.

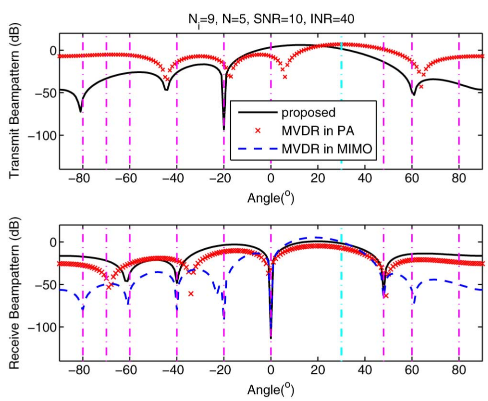

Fig. 3. Transmit and receive beampatterns for $N_i = 9$.

It is found that the LCMV beamformer does not outperform the MVDR beamformer in the output SINR. This phenomenon is consistent with the theoretical results in [15]. Comparisons between the simulation results obtained with LCMV beamformers and those obtained with the proposed algorithm yield the same conclusion as in Fig. 1. Therefore, these simulation results of the LCMV beamformers are not reported here.

In the following, the transmit and receive beampatterns are presented for different N_i. Due to space limitation, we only illustrate the cases of $N_i = 5$ and 9 which correspond to Figs. 2 and 3, respectively. Note that the transmit beampattern of the omnidirectional MIMO radar is not presented here, since it is just a horizontal line due to the omnidirectional transmission.

Inspection of Fig. 2 highlights that the proposed algorithm can produce nulls near the DOAs of 5 interference signals at either the transmit side or the receive side. In contrast, nulls generated by the PA radar are not consistent with the DOAs of 5 interference signals, and the nulls' locations in the transmit beampattern of the PA radar are fixed, and cannot be adjusted toward the DOAs of the interference signals. For the MIMO radar, it can also effectively form nulls near the DOAs of 5 interference signals. However, the echo power of the target in the MIMO radar is weak with respect to the system descried in Section II due to the omnidirectional transmission. Therefore, the MVDR beamformer in the MIMO radar performs worse than the proposed algorithm.

In Fig. 3 with $N_i = 9$, as expected, each of all algorithms considered here can only generate at most 8 nulls, and thus at least one interference cannot be effectively eliminated. Additionally, the directions of some of these nulls formed by the proposed algorithm are not perfectly towards the DOAs of the interference signals. Therefore, the proposed algorithm suffers from significant degradation in the output SINR when the powers of the interference signals are strong.

V. Conclusion

A sequential optimization algorithm is proposed to design both transmit beamforming and receive filter for achieving the maximum output SINR in an active array. Numerical results show that compared with the MVDR or LCMV beamformer in the PA radar, our method can handle more interference signals and achieve higher SINR; compared with the MVDR or LCMV beamformer in the omnidirectional MIMO radar, our method obtains a significant output SINR gain. Different from the conventional MDVR and LCMV approaches, where knowledge of the interferences is employed only for receiver design, our approach employs the knowledge for joint transmitter and receiver optimization. This is the reason for the performance improvement.

References

[1] P. Stoica, J. Li, and M. Xue, "Transmit codes and receive filters for radar," *IEEE Signal Process. Mag.*, vol. 25, no. 6, pp. 94–109, Nov. 2008.

[2] A. Aubry, A. De Maio, A. Farina, and M. Wicks, "Knowledge-aided (potentially cognitive) transmit signal and receive filter design in signal-dependent clutter," *IEEE Trans. Aerosp. Electron. Syst.*, vol. 49, no. 1, pp. 93–117, Jan. 2013.

[3] A. De Maio, S. De Nicola, Y. Huang, S. Zhang, and A. Farina, "Code design to optimize radar detection performance under accuracy and similarity constraints," *IEEE Trans. Signal Process.*, vol. 56, no. 11, pp. 5618–5629, Nov. 2008.

[4] A. De Maio, S. De Nicola, Y. Huang, Z.-Q. Luo, and S. Zhang, "Design of phase codes for radar performance optimization with a similarity constraint," *IEEE Trans. Signal Process.*, vol. 57, no. 2, pp. 610–621, Feb. 2009.

[5] A. De Maio, Y. Huang, M. Piezzo, S. Zhang, and A. Farina, "Design of optimized radar codes with a peak to average power ratio constraint," *IEEE Trans. Signal Process.*, vol. 59, no. 6, pp. 2683–2697, Jun. 2011.

[6] P. Stoica, H. He, and J. Li, "Optimization of the receive filter and transmit sequence for active sensing," *IEEE Trans. Signal Process.*, vol. 60, no. 4, pp. 1730–1740, Apr. 2012.

[7] J. Li and P. Stoica, "The phased array is the maximum snr active array [lecture notes]," *IEEE Signal Process. Mag.*, vol. 27, no. 2, pp. 143–144, Mar. 2009.

[8] P. Stoica and R. L. Moses, *Introduction to Spectral Analysis*. Upper Saddle River, NJ, USA: Prentice-Hall, 1997.

[9] H. Li and B. Himed, "Transmit subaperturing for MIMO radars with co-located antennas," *IEEE J. Sel. Topics Signal Process.*, vol. 4, no. 1, pp. 55–65, Feb. 2010.

[10] C.-Y. Chen and P. P. Vaidyanathan, "MIMO radar waveform optimization with prior information of the extended target and clutter," *IEEE Trans. Signal Process.*, vol. 57, no. 9, pp. 3533–3544, Sep. 2009.

[11] J. Capon, "High resolution frequency-wavenumber spectrum analysis," *Proc. IEEE*, vol. 57, no. 8, pp. 1408–1418, Aug. 1969.

[12] G. H. Golub and C. F. Van Loan, *Matrix Computations*, 3rd ed. ed. Baltimore, MD, USA: Johns Hopkins Univ. Press, 1996.

[13] O. L. Frost, III, "An algorithm for linearly constrained adaptive array processing," *Proc. IEEE*, vol. 60, no. 8, pp. 926–935, Aug. 1972.

[14] R. T. Hoctor and S. A. Kassam, "The unifying role of the coarray in aperture synthesis for coherent and incoherent imaging," *Proc. IEEE*, vol. 78, no. 4, pp. 735–752, Apr. 1990.

[15] M. Souden, J. Benesty, and S. Affes, "A study of the LCMV and MVDR noise reduction filters," *IEEE Trans. Signal Process.*, vol. 58, no. 9, pp. 4925–4935, Sep. 2010.